Marquette University
e-Publications@Marquette

Electrical and Computer Engineering Faculty Research and Publications

Electrical and Computer Engineering, Department of

2-11-2015

Using Cross-Linked SU-8 to Flip-Chip Bond, Assemble, and Package MEMS Devices

Robert A. Lake
Air Force Institute of Technology

Ronald A. Coutu Jr.
Marquette University, ronald.coutu@marquette.edu

Electrical and Computer Engineering Faculty Research and Publications/College of Engineering

Contents

Using Cross-Linked SU-8 to Flip-Chip Bond, Assemble, and Package MEMS Devices

Robert A. Lake
Department of Electrical and Computer Engineering, Air Force Institute of Technology, Wright-Patterson AFB, OH

Ronald A. Coutu
Department of Electrical and Computer Engineering, Air Force Institute of Technology, Wright-Patterson AFB, OH

Abstract:

This paper investigates using an SU-8 photoresist as an adhesive material for flip-chip bonding, assembling, and packaging microelectromechanical systems devices. An important factor, when using SU-8 as an adhesive material is to control ultraviolet (UV) exposure during fabrication to maximize bond strength due to material cross linking. This approach is much improved over previous efforts where SU-8 bake times and temperatures where changed to alter material cross-linking. In this paper, bake times and temperatures were maintained constant and total UV exposure energy was varied. Once fabricated, bond strength was systematically tested to determine the tensile loads needed to separate bonded structures. The resulting separation force was shown to increase with UV exposure and ranged from 0.25 (5-s exposure) to 1.25 N (15-s exposure). The separation test data were then analyzed to determine the statistical significance of varying UV exposure time and its effect on SU-8 cross-linking and bond strength. The data show that total UV exposure dose is directly correlated with the bond strength of SU-8 bonded structures. By varying only UV dose, the separation force data exhibited a statistically significant dependence on SU-8 cross linking with a 5% probability of error. Further, SU-8 etch resiliency increased by approximately 40%-60% as cross linking was increased with UV exposures ranging from 5 to 15 s.

SECTION I. Introduction

SU-8 is a thick, high-contrast, epoxy-based, negative tone photoresist commonly used in micromachining high-aspect-ratio microelectromechanical system (MEMS) devices and in other microelectronics applications.[1] Through ultraviolet (UV) exposure and postexposure bake (PEB) steps SU-8 layers become cross-linked, robust, and resistant to standard developers and also etching methods (O_2 plasma ashing, reactive ion etching, corrosive chemistry etches, and so on). These unique properties make SU-8 an excellent masking material when fabricating MEMS devices. During processing, the exposure step creates an acid and the PEB thermally activates the acid and promotes material cross-linking of the exposed areas. SU-8 is commonly used in microfluidics, nanoimprint lithography, and other applications that require advanced photolithography techniques.[2] The advantages of using SU-8 include: biocompatibility, low levels of outgassing when used in vacuum, thermal stability, and highly robust films/structures suitable for harsh, corrosive environments.[3] This paper investigates SU-8 cross-linking and its effects on bond strength and etch resiliency. The challenge in this paper was showing a

statistically significant correlation between SU-8 cross-linking and bond strength suitable for assembling and packaging devices.

Many MEMS devices, especially those with complex mechanisms, require protection or operation within a vacuum or hermetic environment. Due to their fragile nature, movable parts or specific operation atmosphere requirements, standard microelectronic packaging technologies cannot typically be used with MEMS.[4] Wafer bonding, however, is commonly used in MEMS using processes such as: fusion bonding,[5] anodic bonding,[6] eutectic bonding,[7,8] glass frit bonding,[9] and polymer bonding.[10] The main difference between these methods is the material used as the bonding agent. A common trait to all of these methods, however, is the need for high pressures and temperatures to successfully make the bond. Some of these methods require temperatures over 1000 °C to attain adequate bond strengths necessary for device packaging. These high temperatures can damage MEMS and other devices while they are being encapsulated or packaged.[11] Low-temperature bonding methods are critical to minimizing component damage due to assembly and packaging processes.

Besides its application as a masking or mold material, when etching or forming high-aspect structural layers, SU-8 can also be used as an adhesive material when flip-bonding, assembling, or packaging devices. The advantages of using SU-8 as a bonding material include: low-bonding temperature, ease of processing, low cost, near hermetic seal, and conformal sealing.[12] In addition, bonding with a patternable polymer, such as SU-8, reduces residual stress in the packaged components, minimizes damage caused from high electric fields, and lowers negative effects caused by high-temperature processing.[13] Two prior research efforts have investigated using SU-8 as an adhesive material in flip-chip bonding.[14,15] The first study by Ochoa *et al.*[14] used manufacturer-recommended bake times and temperatures to process 50 μ m ×50 μ m SU-8 bond pad areas that were 2-μ m thick. Bond strength was not measured or quantified and was assessed based on how well the resulting flip-bonded optical MEMS structures survived further processing. A 30% yield resulted when the flip bonder tip temperature and applied load were set to 135 °C and 1 kg, respectively.[14] Based on Ochoa *et al.*'s qualitative assessment of bond strength, their results cannot be directly applied to nor compared with other bond strength results.

The second study, by Glauvitz *et al.,*[15] investigated SU-8 cross-linking and its effect on material bond strength. In this paper, standard flip-chip bonding protocols were used while the SU-8 manufacturer-recommended two-step PEB process was varied. Specifically, the PEB2 temperature was raised from 95 °C to 110 °C and the bake times were incremented from 1 to 10 min.[15] The modeled raw data exhibited a downward trending separation load versus softbake time. Once the statistical outliers (±4 standard deviations about the mean value) were removed, however, the model failed the two-sided t-test indicating that a statistically significant correlation did not exist (i.e., $R^2 = 2\%$). Nevertheless, preliminary results showed that a 3-min softbake time yielded the highest separation load.[15]

Another important factor when investigating SU-8 bond strength that has not been previously considered is the degree of SU-8 cross-linking caused by UV exposure during device fabrication. In this paper, manufacturer-recommended SU-8 bake times and temperatures were used and UV exposure times (i.e., dose) were varied. Once the test structures were fabricated and flip-bonded together, the SU-8 bonded structures were then systematically tested under tensile loads to determine the separation force needed to break the SU-8 bonds. The resulting data were analyzed and the statistical significance of the UV exposure parameter was examined.

SECTION II. Methodology

A. Test Structure Fabrication

Fabrication of the SU-8 test structures followed the prescribed process flow given by Microchem's SU-8 (2000) processing guidelines shown in Fig. 1.[1]
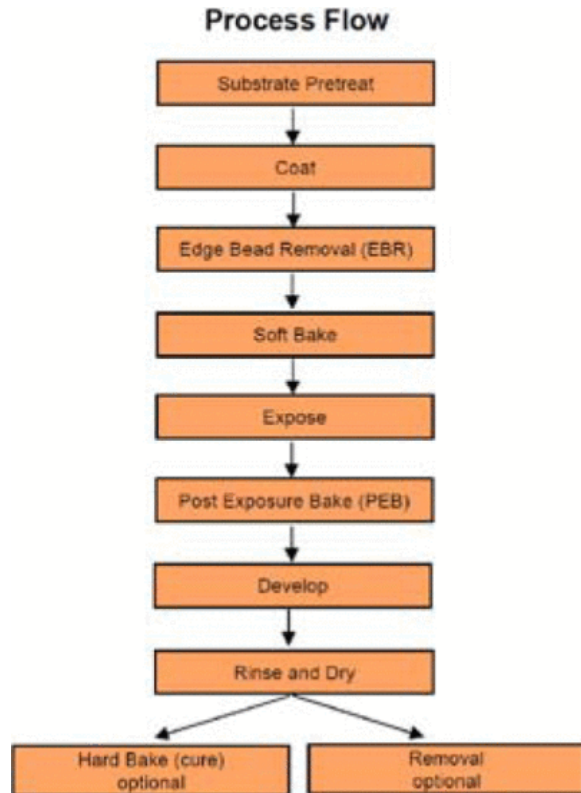
Process Flow

Fig. 1. Process flow for SU-8 fabrication as outlined by Microchem SU-8 datasheet.[1]

All of the processing took place in a class 100/1000 clean room with the temperature and relative humidity maintained at 68 °C and 35%, respectively. During the substrate pretreat processing step, organic contaminants were removed from 3-in, n-type (100) silicon (Si) wafers with acetone, methanol, and deionized water (DIW) sprays for 30 s each followed by a clean, dry N_2 spray. The wafers were then dipped in a 7:1 buffered oxide etch for 1 min to remove the native oxide and maximize SU-8 adhesion to the Si wafer. This ensured that SU-8 adhesion to the Si wafer was greater than the bond strength between the SU-8 test structures that isolated the bond strength of interest. The wafers were then rinsed with DIW for 30 s, dried with N_2, and then heated on a hot plate for 2 min at 110 °C to evaporate any remaining moisture. After cooling for approximately 15 min, the wafers were spin-coated with SU-8 (2002) at 500 r/min for 5 s (i.e., spread cycle) and then 3000 r/min for 30 s (i.e., spin cycle) resulting in a uniform, approximately 5-μ m thick (as shown in Fig. 2) SU-8 layer. Immediately after spin-coating, the wafers were prebaked and softbaked, per manufacturer specifications, for 1 min (65 °C) and 2 min (95 °C), respectively.
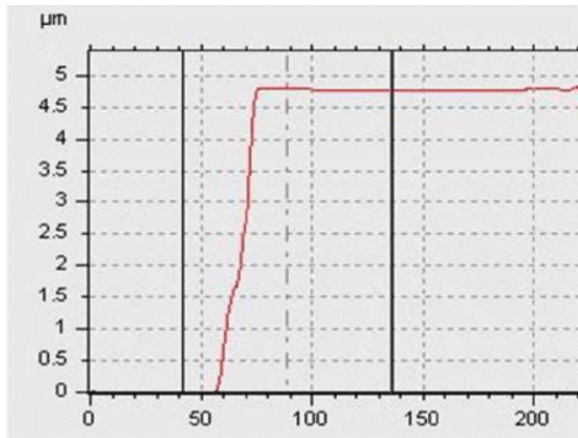
Fig. 2. Representative step height measurement, using a KLA-Tencor Alpha IQ Step profilometer, of an SU-8 test ring with a step height of ~4.7 μ m.

The UV exposure step was accomplished using a Karl Suss MJB3 mask aligner with the power set to 11 mW/cm^2. Exposure times were varied from 5–15 s resulting in total UV energy doses ranging from 55–165 mJ/cm^2. Based on the 5-μ m thick SU-8 layer, an exposure energy of 93.5 mJ/cm^2 was recommended in the SU-8 application guide.[1] This dose was defined in this paper as the 100% dose level and all other doses were determined from this baseline value resulting in exposure doses ranging from 58% to 176% of the recommended energy dose. The bonded test structures, shown in Fig. 3, were square rings 200-μ m wide and 2 mm long, resulting in a total bondable area of 1.44 mm^2.
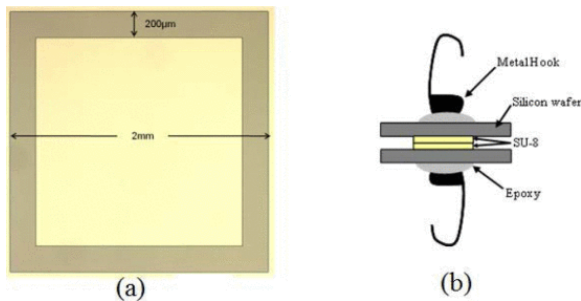

Fig. 3. (a) Optical image of fabricated bond pad, prior to flip-bonding, consisting of a square ring measuring 2 mm×2 mm with a width of 200 μ m. (b) Cross-sectional diagram of the fully assembled test structure ready for tensile testing.

Immediately after UV exposure, the specific degree of sample cross-linking was locked in by transferring the wafer to a hot plate for the manufacturer-recommended two-step PEB process. The samples were then developed for 1 min using a Microchem's SU-8 developer, rinsed in rinses in DIW (30 s) and isopropyl alcohol (IPA—10 s), and dried using clean, dry N$_2$ gas. Finally, the wafers were diced into 6.35 mm ×6.35 mm squares, each containing a square ring (Fig. 3) or one side of a complete test structure that was later flip-bonded to another square ring.

B. Flip Bonding and Test Structure Assembly

Next, the samples were bonded together using a Semiconductor Equipment Corporation Eagle 860 flip-chip bonder. The bonding sequence for all samples was kept constant to ensure that UV exposure was

the only variable varied throughout the process. The preprogrammed bonding sequence had both the tip and stage temperatures set at 125 °C. During the bonding sequence, they were both rapidly heated to 150 °C while a load of 1 kg was applied for 10 s. With flip-bond pressure removed, the stage was rapidly cooled back to 125 °C with flowing N_2. This controlled timing minimized residual temperature effects and inadvertent SU-8 cross-linking due to flip-bonding process. Again, this precaution was taken to ensure that the only variable in the experiment was the level of cross-linking due to the varying UV exposure.

After the SU-8 square rings were flip-chip bonded together, small metal hooks were fixed to outside Si surfaces, as shown in Fig. 3, using a two-part epoxy. The hooks were dipped in the epoxy and then placed in the center of the bonded samples, taking care to align the hooks directly over each other (also shown in Fig. 3). This ensured that the tensile load forces, applied during the separation test sequence, were normal to the bonded structures and that shear loads were minimized. The material used to make the metal hooks was extremely rigid and chosen to minimize flex or stiffness variations during tensile load testing resulting in highly consistent force measurements.

C. Separation Force Testing

A microforce testing system (MTS) Tytron 250, shown in Fig. 4, was used to apply the tensile loads and pull the bonded SU-8 test samples apart.
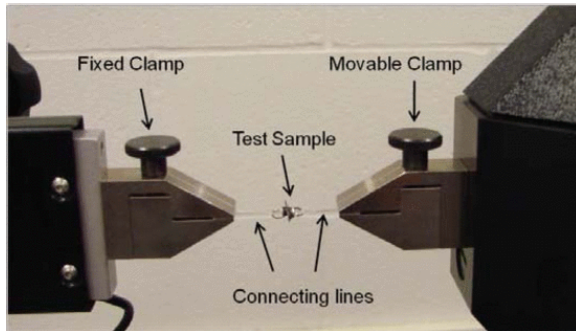

Fig. 4. Fully assembled test sample, mounted in a MTS Tytron 250, during a separation test of a bonded SU-8 test sample.

The MTS Tytron 250 system was configured to perform automated load testing ranging from 0.001 to 44.5 N while recording all necessary data. The test samples were mounted horizontally in the MTS unit between two clamps using a 1-in loop of ultralow stretch braided line to minimize the effects of stiffness variations during testing. The sequence for mounting samples in the system follows.

1. The right movable clamp was commanded to the home position.
2. Braided line loops were then placed onto the sample hooks.
3. The right movable clamp was positioned away from home so that the sample slightly sagged with no measurable axial force.

With the force test ready to begin, the software was configured to pull at a constant rate (1 mm/min) with the force and clamp displacement being measured every 9.77 ms. Fig. 5 is an example test run where an applied tensile load of approximately 1.13 N was required to separate the test sample and break the SU-8 bonds.
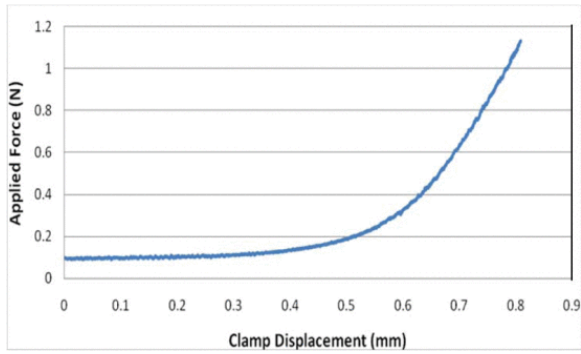
Fig. 5. Graph of the applied force versus clamp displacement showing an SU-8 bonded structure that separated with approximately 1.13 N of applied axial force.

SECTION III. Results and Discussion

A. Raw Data Statistical Analysis

The samples were all tested until the SU-8 bonded structures separated at which time the tensile force was recorded. Statistical analysis of these raw data indicated a direct correlation between UV exposure dose and separation force. A trend-line was fitted to these raw data (Fig. 6) and a two-sided t-test determined, with a 10% probability of error ($\alpha = 0.1$), that the slope of this line was nonzero. The following equation, determined through regression analysis, models the trend-line:

$$Y = 0.0367 + 0.0779X \text{ (1)}$$

where Y is the separation force in newtons and X is the UV exposure time in seconds. This model was found to have a coefficient of correlation (R^2) of 0.31, meaning that 31% of the variability of the separation force can be attributed to the UV exposure dosage.
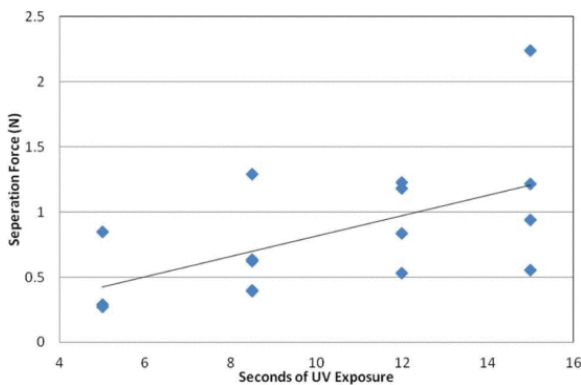

Fig. 6. Predictor trend-line fitted to raw data from the separation testing was found to be nonzero with 90% confidence.

Further examination of the semistudentized residuals revealed a nonconstancy of variance and a nonnormal distribution shown in Fig. 7. This megaphone shape of the residual plot indicates that the error variance is larger for longer UV exposure doses.
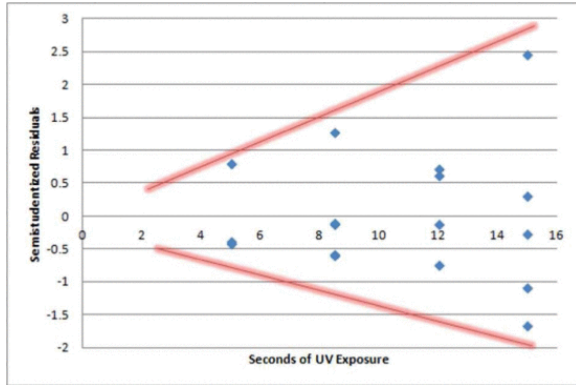
Fig. 7. Plot of the semistudentized residuals versus the predictor variable of UV exposure time indicates a nonconstant error variance. The megaphone shape indicates that the error variance increase as UV exposure times increase.

To investigate the nonconstant variance and nonnormality further, a Box-Cox transformation was performed on the raw data

$$Y' = \frac{Y^{-0.2}-1}{-0.29815} \text{ (2)}$$

where Y' are the transformed data for the separation force and Y is the original separation force. The following equation is the resulting trend-line for the transformed data shown in Fig. 8
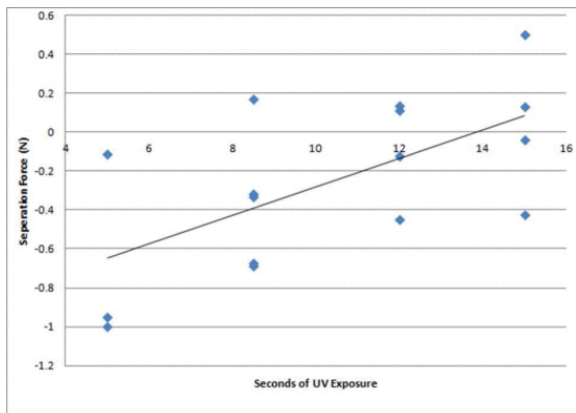
$$Y = -1.0093 + 0.073X. \text{ (3)}$$

Fig. 8. Predictor trend-line fitted to the transformed data of the separation testing was found to be nonzero with 95% confidence.

The new trend-line (Fig. 8), analyzed with a two-sided t -test, corroborated the results of the initial analysis and revealed an improved 5% probability of error ($\alpha = 0.05$) that the original raw data exhibited a nonzero slope. In addition, the new R^2 value was now 0.39, meaning that 39% of the variability of the separation force can be attributed to the UV exposure dose. Residual analysis for this new trend-line model shows a constancy of variance and normal distribution of residuals (Fig. 9), indicating that the inferences made about this model are all valid. Further analysis of the

semistudentized residuals of these transformed data revealed that there were no statistical outliers in the raw data (as was the case with Glauvitz *et al.*'s raw data[15]).
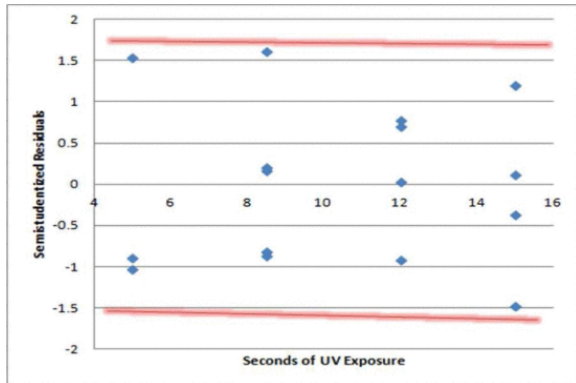

Fig. 9. Plot of the semistudentized residuals of the transformed data versus the predictor variable of UV exposure time shows a constancy of variance, indicating that inferences made about this data set are valid.

Additional analysis of the transformed data reveals that the residuals now fall on a normal distribution (Fig. 10), further emphasizing that the inferences about the nonzero slope of the relation between the UV exposure time and separation force are all valid. A Shapiro-Wilks test was also conducted on these residuals, which indicated that they are normally distributed.
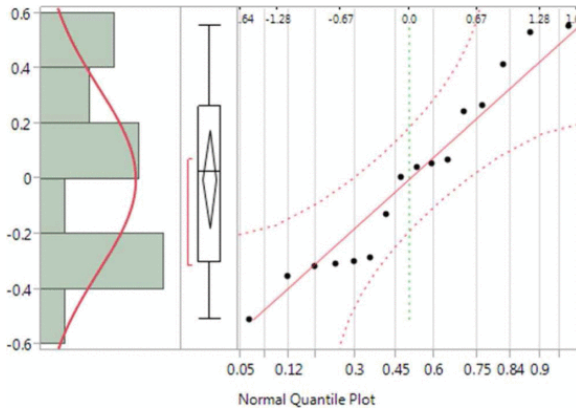

Fig. 10. Distribution plot of the residuals of the transformed data. The close fit of the data points to the line indicates a normalcy of distribution.

A power of test analysis indicated that for a 5% probability of error ($\alpha = 0.05$) and a 39% coefficient of correlation ($R^2 = 0.39$), a sample size of at least 15 was sufficient to draw our conclusions.

Since the only variable examined in this experiment was UV exposure dosage, the remaining 60% cannot be definitively determined; however, we speculate that the remaining variability be attributed to stochastic factors such as PEB temperature variations, film thickness variations, and data collection uncertainty. SU-8 robustness to etching, a necessary attribute for materials used in MEMS fabrication, assembly, and packaging was investigated next.

B. Etch Resiliency of Cross-Linked SU-8

The cross-linked SU-8 materials processed during this paper were further investigated to assess their resiliency to plasma etching. The thicknesses of unbonded, cross-linked SU-8 structures were initially measured using a KLA Tencor Alpha IQ Step surface profilometer. The samples were etched in an O_2 plasma asher for 5 min at 100 W, the film thickness being recorded after etching. The samples were then placed back in the plasma asher for 15 min at 100 W, the subsequent thicknesses of the SU-8 structures being recorded. Five structures were measured for each UV dosage with the plot of SU-8 thicknesses versus dosage shown in Fig. 11.
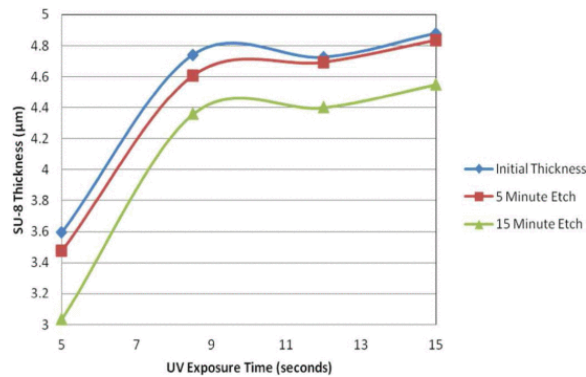

Fig. 11. Plot of the average SU-8 thicknesses with respect to UV exposure time for the initial thickness, following a 5-min oxygen plasma etch, and following a 15-min oxygen plasma etch.

Etch rates were determined by examining the difference between the initial and postetch thicknesses. The overall negative slope of the data shows a lowered thickness delta indicating that increased levels of UV dosage (and higher degrees of cross-linking) resulted in lower etch rates or higher SU-8 etch resiliency. Similar results were observed regardless of the postexposure etch times. The 15-min etch line, shown in Fig. 12, reveals a 37 nm/min etch rate with 5 s of UV exposure and 21 nm/min etch rate with a 15-s exposure resulting in an improved etch resiliency of 43.2%. The 5-min etch line revealed a 58.3% increase in etch resiliency with increased UV exposure.
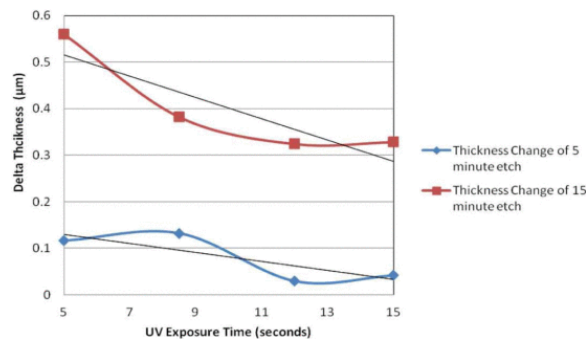

Fig. 12. Plot of the thickness delta as it relates to UV exposure time. The negative slope of the data indicates that higher UV dosages decrease the etch rate of SU-8.

C. Visual Inspection of Pre- and Posttest Structures

Based on the separation force results, the separated test samples were optically imaged to qualitatively assess the actual bond area. Fig. 13(a) is an optical image of a prebonded structure. Fig. 13(b) is the

same structure after the bonding and separation testing. Fig. 13(b) shows material transfer between the upper and lower bondpads indicating areas of high bond strength between structures, demonstrating the connection between the degree of cross-linking and bond strength.
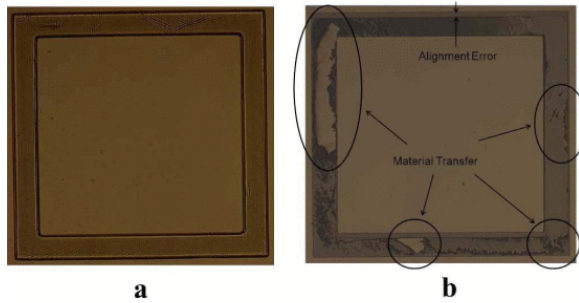

Fig. 13. Optical image of prebonded and posttest SU-8 structures. (a) Prebonded structure. (b) Posttest structure after separation.

SEM images of the SU-8 bondpads taken before [Fig. 14(a)] and after the bonding and separation testing [Fig. 14(b)] reveal deformation of the structures along the edges resulting from the applied pressure during the bonding process.
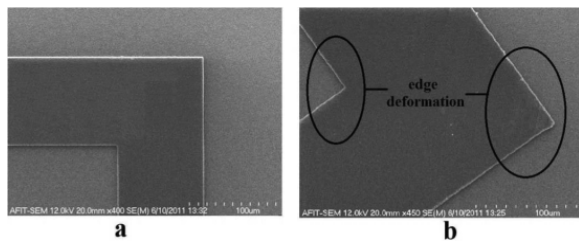

Fig. 14. SEM image of the SU-8 bondpad (a) before and (b) after (bonding and separation shows no indication of edge deformation showing edge deformation of the structure occurring during the process.

SECTION IV. Conclusion

In this paper, we present initial results to quantify the effects of SU-8 cross-linking and its correlation with the bond strength when used as an adhesive material for device assembly and packaging. SU-8 etching resiliency to oxygen plasma etching was also briefly investigated as another means of quantifying SU-8 cross-linking levels. The results show that UV exposure dose is directly correlated with tensile separation force when two structures are flip-chip bonded using SU-8 as the bonding material. By varying only the UV exposure dose, it was clearly shown that cross-linking and therefore bond strength have a statistically significant dependence on UV exposure times. Based on these preliminary results, more highly cross-linked SU-8 appears to demonstrate improved qualities which are key factors in determining the suitability of SU-8 as an adhesive material for flip-chip bonding, assembling, and packaging MEMS and other microelectronic devices.

ACKNOWLEDGMENT

References

1. *SU-8 2000 Permanent Epoxy Photoresist Processing Guidelines*, Apr. 2014, [online] Available: http://www.microchem.com.

2. S. A. Ostrow, R. A. Coutu, "Novel microelectromechanical systems image reversal fabrication process based on robust SU-8 masking layers", *J. Micro/Nanolithogr. MEMS MOEMS*, vol. 10, no. 3, pp. 033016-1-033016-7, 2011.

3. H. Lorenz, M. Despont, N. Fahrni, N. LaBianca, P. Renaud, P. Vettiger, "SU-8: A low-cost negative resist for MEMS", *J. Micromech. Microeng.*, vol. 7, no. 3, pp. 121-124, 1997.

4. M. Shahriar Rahman, M. M. Chitteboyna, D. P. Butler, Z. Celik-Butler, S. P. Pacheco, "Device-level vacuum packaging for RF MEMS", *J. Microelectromech. Syst*, vol. 19, no. 4, pp. 911-918, Aug. 2010.

5. Y. T. Cheng, L. Lin, K. Najafi, "Localized silicon fusion and eutectic bonding for MEMS fabrication and packaging", *J. Microelectromech. Syst.*, vol. 9, no. 1, pp. 3-8, Mar. 2000.

6. B. Lee, S. Seok, K. Chun, "A study on wafer level vacuum packaging for MEMS devices", *J. Micromech. Microeng.*, vol. 13, no. 5, pp. 663, Jun. 2003.

7. J. Mitchel, G. R. Lahiji, K. Najafi, "Encapsulation of vacuum sensors in a wafer level package using a gold-silicon eutectic", *Proc. 13th Int. Conf. Solid-State Sensors Actuat. Microsyst.*, pp. 928-931, Jun. 2005.

8. J. Mitchel, G. R. Lahiji, K. Najafi, "An improved performance poly-Si Pirani vacuum gauge using heat-distributing structural supports", *J. Microelectromech. Syst.*, vol. 17, no. 1, pp. 93-102, Feb. 2008.

9. D. Sparks, S. Massoud-Ansari, K. Najafi, "Long-term evaluation of hermetically glass frit sealed silicon to Pyrex wafers with feedthroughs", *J. Micromech. Microeng.*, vol. 15, no. 8, pp. 1560, Nov. 2000.

10. H. Kim, K. Najafi, "Characterization of low-temperature wafer bonding using thin-film parylene", *J. Microelectromech. Syst.*, vol. 14, no. 6, pp. 1347-1355, Dec. 2005.

11. L. Lin, "MEMS post-packaging by localized heating and bonding", *IEEE Trans. Adv. Packag.*, vol. 23, no. 4, pp. 608-616, Nov. 2000.

12. C. Wang, A. Brown, I. De Wolf, "Low temperature polymer bonding processes for MEMS encapsulation", Sep. 2007.

13. C.-T. Pan, H. Yang, S.-C. Shen, M.-C. Chou, H.-P. Chou, "A low-temperature wafer bonding technique using patternable materials", *J. Micromech. Microeng.*, vol. 12, no. 5, pp. 611-615, 2002.

14. E. Ochoa et al., " Flip bonding with SU-8 for hybrid Al x Ga 1- x As-polysilicon MEMs-tunable filter ", *J. Micro./Nanolith. MEMS/MOEMS*, vol. 6, no. 3, pp. 033007, Jul./Sep. 2007.

15. N. E. Glauvitz, L. A. Starman, R. A. Coutu, R. L. Johnston, "Effects of SU-8 cross-linking on flip-chip bond strength when assembling and packaging MEMS", *Proc. Eug.*, vol. 25, pp. 471-474, Dec. 2011.